

Magnetic flares in Active Galactic Nuclei: Modeling the iron $K\alpha$ -line

R. W. Goosmann^{1,2,*}, B. Czerny³, M. Mouchet^{2,4}, V. Karas¹, M. Dovčiak¹, G. Ponti^{5,6}, A. Różańska³, and A.-M. Dumont²

¹ Astronomical Institute of the Academy of Sciences, Boční II 1401, CZ–14131 Prague, Czech Republic

² Observatoire de Paris, Section de Meudon, LUTH, 5 place Jules Janssen, F–92195 Meudon Cedex, France

³ Nicolaus Copernicus Astronomical Center, Bartycka 18, 00-716 Warsaw, Poland

⁴ Laboratoire Astroparticule et Cosmologie, Université Denis Diderot, 2 place Jussieu, 75251 Paris Cedex 05, France

⁵ Dipartimento di Astronomia, Università di Bologna, Via Ranzani 1, I–40127 Bologna, Italy

⁶ INAF–IASF Bologna, via Gobetti 101, I–40129, Bologna, Italy

Received 30 Aug 2006, accepted —

Published online later

Key words accretion, accretion disks; galaxies: active; radiative transfer; relativity; X-rays: galaxies

The X-ray spectra of Active Galactic Nuclei (AGN) are complex and vary rapidly in time as seen in recent observations. Magnetic flares above the accretion disk can account for the extreme variability of AGN. They also explain the observed iron $K\alpha$ fluorescence lines. We present radiative transfer modeling of the X-ray reflection due to emission from magnetic flares close to the marginally stable orbit. The hard X-ray primary radiation coming from the flare source illuminates the accretion disk. A Compton reflection/reprocessed component coming from the disk surface is computed for different emission directions. We assume that the density structure remains adjusted to the hydrostatic equilibrium without external illumination because the flare duration is only a quarter-orbit. The model takes into account the variations of the incident radiation across the hot spot underneath the flare source. The integrated spectrum seen by a distant observer is computed for flares at different orbital phases close to the marginally stable orbit of a Schwarzschild black hole and of a maximally rotating Kerr black hole. The calculations include relativistic and Doppler corrections of the spectra using a ray tracing technique. We explore the practical possibilities to map out the azimuthal irradiation pattern of the inner accretion disks and conclude that the next generation of X-ray satellites should reveal this structure from iron $K\alpha$ line profiles and X-ray lightcurves.

© 2006 WILEY-VCH Verlag GmbH & Co. KGaA, Weinheim

1 Introduction

X-ray spectra of active galactic nuclei (AGN) are dominated by a power-law shape with an exponential cutoff at several hundred keV. They frequently show additional features, such as a soft-excess and signs of warm absorption. The observed iron $K\alpha$ emission line and the Compton hump in many AGN indicate a mechanism for X-ray reprocessing. It is widely believed that the power-law component, i.e. the so-called primary radiation, emerges by Comptonization in a hot plasma above the disk and is partly reprocessed by the relatively colder disk atmosphere.

The iron $K\alpha$ line is particularly important to investigate the inner parts of the accretion flow around black holes. The high cosmic abundance of iron, together with a relatively high fluorescence yield, give rise to strong $K\alpha$ line emission. The overall line is actually a superposition of lines from different ionization states. On top of that, several effects smear the line shape out, e.g. Comptonization inside the upper layers of the accretion disk, or relativistic and Doppler modifications in the vicinity of the black hole (see Fabian et al. 2000 or Reynolds & Nowak 2003 for reviews).

Using theoretical modeling, the observed shape of the iron $K\alpha$ line can be connected to global parameters of the object. The relativistic broadening constrains the black hole spin, the radial emissivity profile of the disk, and the inclination of the object. But also the “local appearance” of the line, i.e. the line profile as it would be seen by an observer co-rotating with the disk, plays a role. This local profile is determined by the energy dissipation within the hot plasma and by the structure of the disk.

In this paper we present theoretical modeling of the iron $K\alpha$ line within the frame work of the magnetic flare model (see e.g. Collin et al. 2003). This model assumes that the hot plasma producing the primary radiation arises from magnetic reconnection events above the accretion disk. We consider orbiting flare sources close to the last stable orbit of a Schwarzschild or a maximally rotating Kerr black hole and we analyze the spectral appearance and the observed lightcurves for different azimuthal phases of the orbit.

2 Model

The flare model for black hole accretion disks was originally suggested by Galeev, Rosner, & Vaiana (1979) and then developed in several papers, such as Haardt, Maraschi,

* e-mail: goosmann@astro.cas.cz

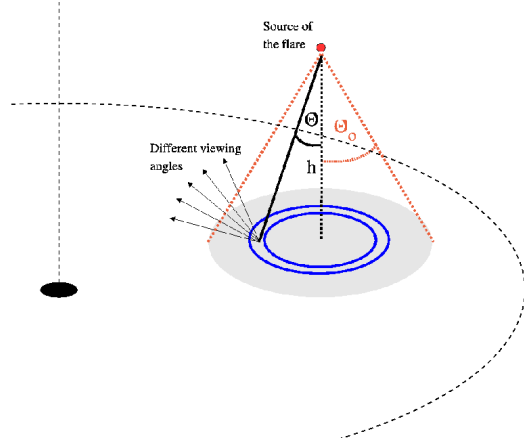


Fig. 1 Illustration of the geometrical setup for the flare model. The scale of the flare geometry is exaggerated for clarity.

& Ghisellini (1994). Here we are specifically interested in the reprocessed component and not in the primary emission directly seen by a distant observer. This reprocessing has been extensively modeled in the past and nowadays the models include a detailed treatment for the hydrostatic equilibrium of the disk (see e.g. Nayakshin, Kazanas, & Kallman 2000; Ballantyne, Ross, & Fabian 2001; Rózańska et al. 2002). Recently, we added some more sophistication to the modeling by including the horizontal structure of the irradiated spot underneath the compact flare source. This is illustrated in Fig. 1.

The hot-spot is defined by the height of the flare source above the disk and by the half-opening angle $\theta_0 = 60^\circ$. We divide the spot into 5 concentric rings and for each of the rings we conduct multi-angle radiative transfer modeling using the codes TITAN and NOAR (Dumont et al. 2000, 2003) in plan-parallel geometry. The primary radiation for each ring is adjusted for the incident angle and for the illuminating flux as given by the distance to the point source. A black body component for the accretion disk is added. We assume that the flare exists for a quarter of an orbit and evaluate it at four different azimuthal phases. The flare duration is significantly shorter than the dynamical time-scale of the disk and thus the hydrostatic equilibrium of the atmosphere should not change over the flare period. Therefore, the vertical disk profile is computed without external illumination using a modified version of the code given in Rózańska et al. (2002). The new version includes corrections for the disk structure due to general relativity. The incident radiation coming from the flare is by a factor of 144 stronger than the thermal emission from the accretion disk. We compute locally emitted spectra for a hot spot at $R = 7 R_g$, defining $R_g = \frac{GM}{c^2}$, from a non-rotating black hole with $M = 10^8 M_\odot$. Relativistic and Doppler effects on the radiation are included by using the ray-tracing code KY (Dovčiak et al. 2004, Dovčiak 2004). It takes into account the Doppler velocity due to the orbital motion of the hot spot and also the intrinsic time evolution of the emitted light.

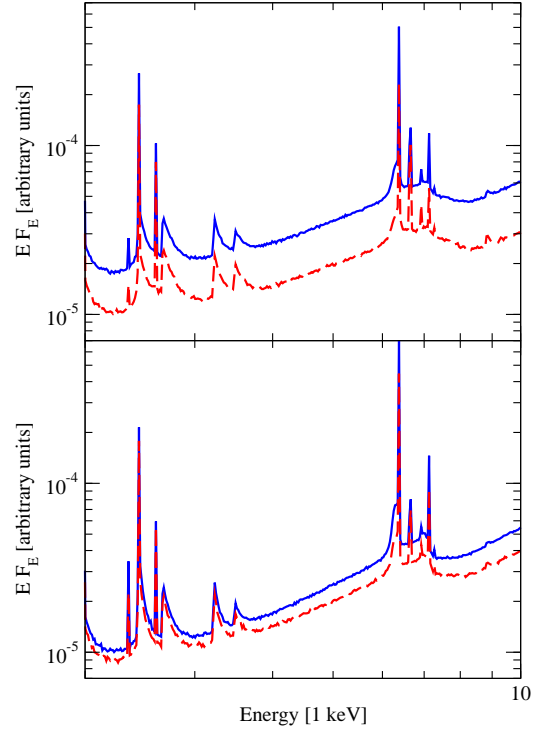


Fig. 2 Local reprocessed spectra coming from different locations within the illuminated spot at $7 R_g$. The top panel corresponds to the spot center and the bottom panel to the spot rim. In each panel the two curves denote local emission angles of $\psi = 10^\circ$ (blue, solid) and $\psi = 60^\circ$ (red, dashed), respectively. The emission angle is measured with respect to the disk normal.

Here we assume that the primary source is switched on and off instantaneously. The reprocessed emission evolves from the center of the spot to the rim. For further details of the computations see Goosmann 2006 or Goosmann et al. (in preparation).

3 Results

Local reprocessed spectra are shown in Fig. 2 for the spot center and the rim at two different local emission angles. A difference in temperature between the two locations in the spot can be inferred from the spectral slopes and the relative strength of the components of the $K\alpha$ -line. From left to right the “neutral” line at 6.4 keV, the helium-like line at 6.7 keV and the hydrogen-like line at 6.9 keV can be seen. The fourth component represents $K\beta$ line emission. At the spot rim the material is colder due to less incident flux. The local emission along the disk normal has a harder spectrum than emission at more grazing angles.

The reprocessed spectra seen by a distant observer are plotted in Fig. 3 for a Schwarzschild black hole ($a/M = 0$) at a radial distance of $7 R_g$ and for the maximally rotating Kerr case ($a/M = 0.998$) at a distance of $3 R_g$. Note that for the Kerr case the computations are not entirely consis-

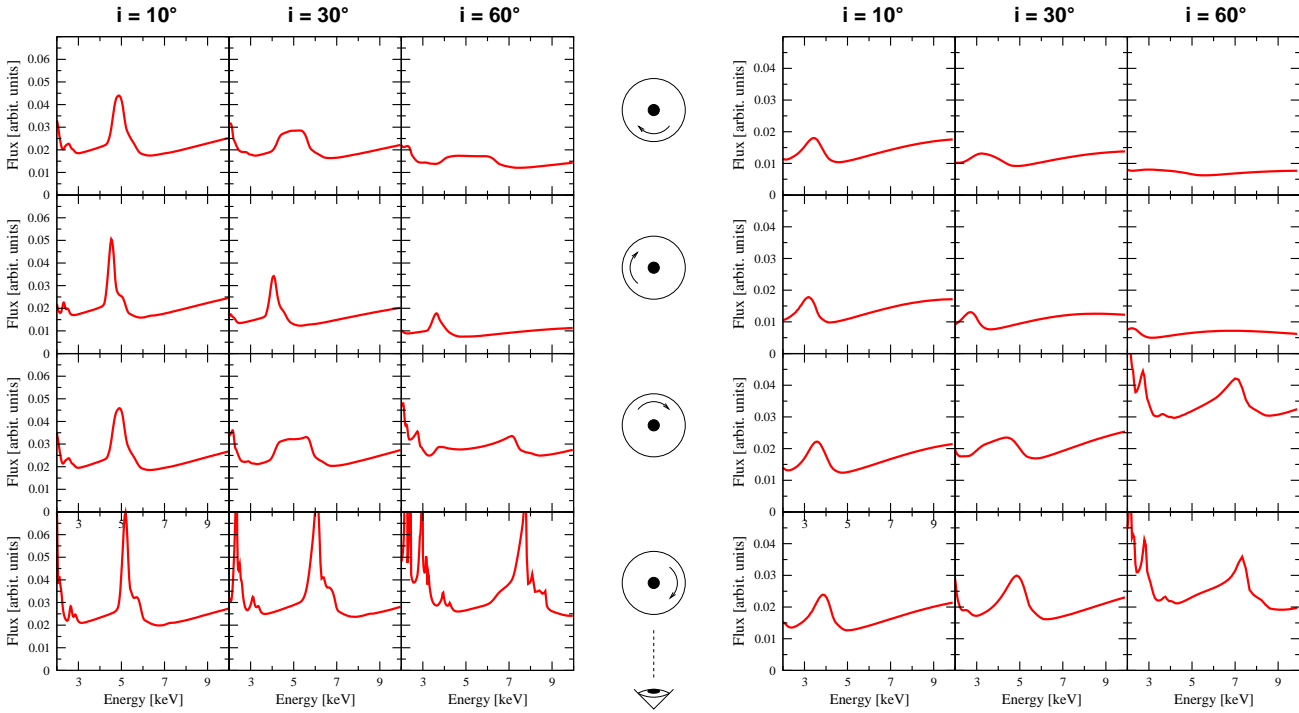


Fig. 3 Integrated reprocessed spectra as seen by a distant observer for a hot-spot completing a quarter-orbit close to the marginally stable orbit of a black hole. The left part of the figure shows the results for a Schwarzschild black hole and a hot spot at $7 R_g$, the right part for an extreme Kerr black hole with $a/M = 0.998$ and a hot spot at $3 R_g$. The 4 rows of diagrams represent different azimuthal directions corresponding to the central illustrations. As indicated, the three columns of each side stand for various inclinations of the distant observer with respect to the disk normal.

tent as we use again the local spectra for the Schwarzschild black hole shown in Fig. 2. The differences seen between the two cases plotted in Fig. 3 are thus entirely due to the general relativistic and Doppler effects. We applied the relativistic corrections only to the reprocessed component and neglected the light-bending acting on the incident radiation during the passage between the source and the disk. The incident light rays are approximated by straight lines. This is sufficiently precise for our cases, as the height of the source above the disk is only $0.5 R_g$ (see Goosmann 2006 or Goosmann et al., in preparation).

While both flare locations are close to the marginally stable orbit, the $K\alpha$ line is more strongly smeared and gravitationally red-shifted for the Kerr black hole. However, for both cases the individual line components are hardly recognizable at any azimuthal angle. The orbital velocity of the spot is higher at $3 R_g$ than at $7 R_g$, which leads to a stronger Doppler shift of the radiation at higher inclinations. The lensing effect is barely relevant for any of the cases considered here because the inclination remains moderate ($i \leq 60^\circ$), i.e. the spot is not close to being lined up with the black hole and the observer.

In Fig. 4 we present the lightcurves corresponding to the spectra of Fig. 3. The overall shape of the lightcurves is similar for both rotation states of the black hole, especially at low inclinations. However, for a given viewing angle the curves differ significantly for different azimuthal positions

of the spot. The timescale for the evolution of the flare emission across the spot is roughly given by the height of the source above the disk $H = 0.5 R_g$. It therefore corresponds to a light traveling time of ~ 250 s for $M = 10^8 M_\odot$. The evolution of the local flare emission across the spot is visible in particular for the rotating black hole. It induces a slight curvature during the rise and the drop of the lightcurves in Fig. 4, while the time evolution of the incident radiation is defined to be box-shaped.

4 Discussion and Conclusion

We have modeled the spectral shape of the iron $K\alpha$ line and the time evolution of the X-ray reprocessing for a magnetic flare occurring close to the marginally stable orbit of a Schwarzschild or a maximally rotating Kerr black hole. Fig. 3 and 4 show that, in principle, the azimuthal location of the reprocessing site close to the last stable orbit can be effectively constrained for both the Schwarzschild and the extreme Kerr case. At a given inclination there are differences in the position of the line centroid caused by Doppler and gravitational shifts. Also, the line profile and the lightcurve are modified by the various relativistic and Doppler effects.

In our model we assume a flare duration of a quarter-orbit. The orbital period at a distance R from a spinning

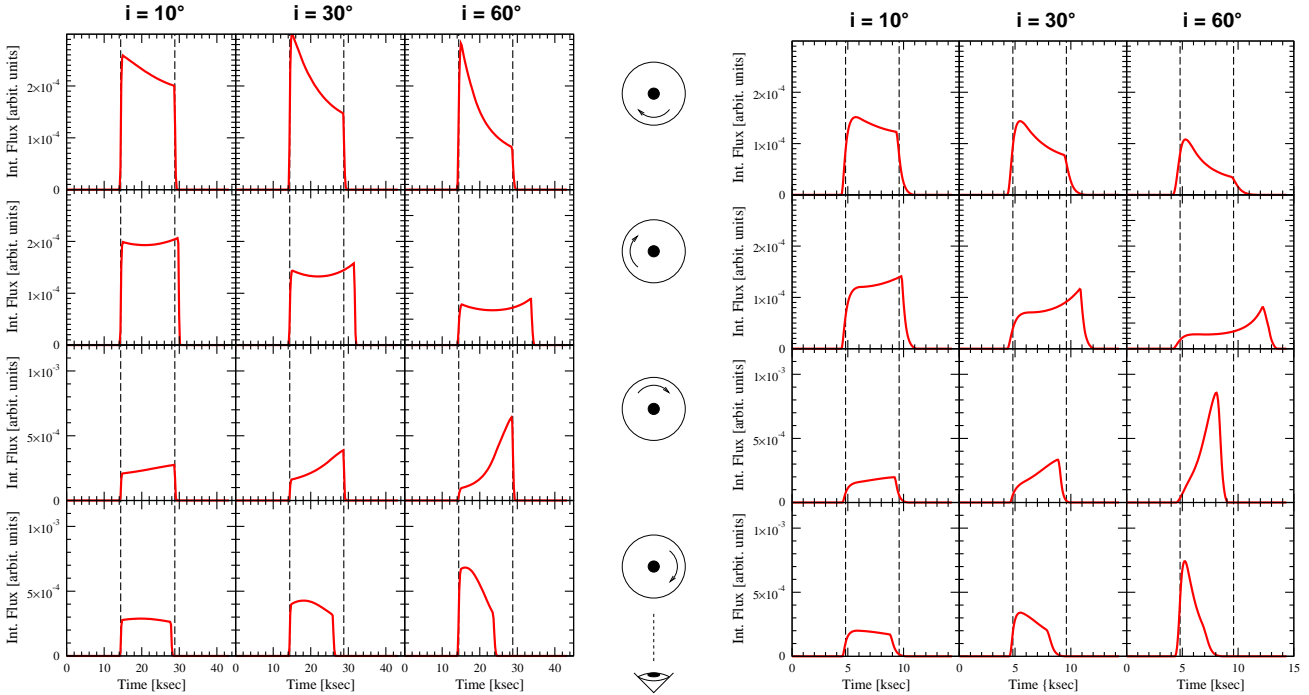


Fig. 4 Lightcurves corresponding to the model spectra shown in Fig. 3. They were integrated over the energy range of 2–10 keV. The vertical dashed lines mark the beginning and the end of the flare irradiation at the spot center as measured by the distant observer. The plots are organized as in Fig. 3. Note, that the vertical scale differs between the two upper and the two lower rows.

black hole with the normalized spin parameter a is given by (see the review by Vladimír Karas in this volume):

$$T_{\text{orbit}} = 3.10 \times 10^3 \frac{M}{M_8} \left[\left(\frac{R}{R_g} \right)^{\frac{3}{2}} + a \right] \text{ [s]}, \quad (1)$$

with the mass M given in units of $M_8 = 10^8 M_\odot$. One derives from equation (1) that our parameter values correspond to the following observation times:

$$T_{\text{quart}}^{\text{Schw}} = 1.44 \times 10^4 \frac{M}{M_8} \text{ [s]} \text{ for } R = 7 R_g, \frac{a}{M} = 0,$$

$$T_{\text{quart}}^{\text{Kerr}} = 0.48 \times 10^4 \frac{M}{M_8} \text{ [s]} \text{ for } R = 3 R_g, \frac{a}{M} = 0.998.$$

With current X-ray satellites observing nearby Seyfert galaxies with high count-rates a sufficiently detailed shape of the iron line requires observation times of ~ 20 ksec or more. Therefore, a flare at $3 R_g$ lasting for a quarter of an orbit cannot be observed yet. The observational limit might be obtained for massive black holes and slightly larger radii though. The next generation of X-ray satellites like XEUS or CONSTELLATION-X is planned to have much larger effective collecting areas. These missions should therefore allow to map out the innermost azimuthal irradiation pattern of some AGN accretion disks.

Meanwhile, variability modeling is another possibility to compare the type of radiative transfer calculations presented here to observed data. An example is given in Goosmann et al. (2006), where we model the rms variability spectrum of the Seyfert galaxy MCG-6-30-15. The modeling

confirms that the central black hole in this object is rapidly spinning and that the radial profile of energy generation in the hot corona of the accretion disk must rise steeply toward the disk center. Further steps in this line of research are possible when including also the power density spectrum that has become available for some nearby Seyfert galaxies such as NGC 3516 (Edelson et al. 1999), NGC 4051 (McHardy et al. 2004), or MCG-6-30-15 (McHardy et al. 2005).

Acknowledgements. This research was supported by the Center for Theoretical Astrophysics in Prague and by the Polish research grant 1P03D00829. RWG also thanks the Hans-Böckler-Stiftung.

References

- Ballantyne, D.R., Ross, R.R., Fabian, A.C. 2001: MNRAS, 327, 10
- Collin, S., Coupé, S., Dumont, A.-M., Petrucci, P.-O., Róžańska, A. 2003: A&A, 400, 437
- Dovčiak, M. 2004: PhD thesis, Charles University, Prague
- Dovčiak, M., Karas, V., & Yaqoob, T. 2004: ApJS, 153, 205
- Dumont, A.-M., Collin, S., Paletou, F., Coupé, S., Godet, O., Pelat, D. 2003: A&A, 407, 13
- Dumont, A.-M., Abrassart, A., Collin, S. 2000: A&A, 357, 823
- Edelson, R., & Nandra, K. 1999: ApJ, 514, 682
- Fabian, A.C., Iwasawa, K., Reynolds, C.S., & Young, A.J. 2000: PASP, 112, 1145
- Galeev, A.A., Rosner, R., Vaiana, G.S. 1979: ApJ, 229, 318
- Goosmann, R.W. 2006: PhD thesis, Universität Hamburg
- Goosmann, R.W. et al. 2006: A&A, 454, 741
- Haardt, F., Maraschi, L., Ghisellini, G. 1994: ApJ, 432, L95

- McHardy, I. M., Gunn, K. F., Uttley, P., & Goad, M. R. 2005: MNRAS, 359, 1469
- McHardy, I. M., Papadakis, I. E., Uttley, P., Page, M. J., & Mason, K. O. 2004: MNRAS, 348, 783
- Nayakshin, S., Kazanas, D., Kallman, T.R. 2000: ApJ, 537, 833
- Reynolds, C.S., Nowak, M.A. 2003: Phys. Rep., 377, 389
- Różańska, A., Dumont, A.-M., Czerny, B., Collin, S. 2002: MNRAS, 332, 799